Contribution from the Department of Chemistry and Biochemistry, University of Colorado, Boulder, Colorado 80309-0215, and Department of Chemistry, D-006, University of California at San Diego, La Jolla, California 92093

Studies on Bis(catecholato)iron(III) Complexes. Structure and Bonding in Members of the Fe(bpy)(Cl_4SQ)(Cl_4Cat)/Fe(bpy)(Cl_4Cat)$_2^-$ Redox Couple

Ding Zirong,[1,2] Samaresh Bhattacharya,[1] James K. McCusker,[3] Paula M. Hagen,[3] David N. Hendrickson,*[,3] and Cortlandt G. Pierpont*[,1]

Received June 13, 1991

Studies have been carried out on complexes of iron-containing two tetrachloro-1,2-benzoquinone ligands bonded with the metal in either the semiquinonate (Cl_4SQ), catecholate (Cl_4Cat), or partially protonated catecholate (HCl_4Cat) forms. The mixed-charge ligand complex Fe(bpy)(Cl_4SQ)(Cl_4Cat) has been prepared by the addition of 2,2'-bipyridine to Fe(Cl_4SQ)$_3$. Mossbauer spectra recorded over the temperature range from 134 to 300 K can be fit to a single quadrupole-split doublet with hyperfine parameters characteristic of high-spin Fe(III). Magnetic measurements carried out over the temperature range from 300 to 9.39 K show that the magnetic moment remains approximately constant at 5.4 μ_B upon decreasing temperature to 50 K. At this temperature there is an increase, possibly resulting from intermolecular ferromagnetic interactions. Magnetic properties of the complex reflect strong intramolecular antiferromagnetic exchange between the high-spin ferric ion and the coordinated radical semiquinone ligand. The Fe(bpy)(Cl_4Cat)$_2^-$ anion has been prepared as the $CoCp_2^+$ salt by one-electron reduction of Fe(bpy)(Cl_4SQ)(Cl_4Cat) or as the PPh_4^+ salt by direct addition of deprotonated catechol and bpy to Fe^{3+}. Crystals of (PPh_4)[Fe(bpy)(Cl_4Cat)$_2$], obtained as the CH_2Cl_2 solvate, form in the triclinic space group $P\bar{1}$ with $Z = 2$ in a unit cell of dimensions $a = 9.633$ (2) Å, $b = 13.868$ (3) Å, $c = 19.543$ (3) Å, $\alpha = 70.99$ (2)°, $\beta = 89.11$ (2)°, $\gamma = 79.78$ (2)°, and $V = 2426.7$ (9) Å^3 with $R = 0.062$ and $R_w = 0.074$. The complex anion is octahedral in structure, with chelated bpy and Cl_4Cat ligands. Carbon-oxygen bond lengths of the Cl_4Cat ligands average to 1.320 (8) Å, a value that is intermediate between typical C-O lengths of semiquinone and catecholate ligands. Mossbauer spectra clearly indicate that the metal is high-spin ferric iron, however. The magnetic moment for the complex shows an unusual temperature dependence, increasing steadily from 6.09 μ_B at 302 K to 6.31 μ_B at 8.00 K. Crystals of Fe($OPPh_3$)$_3$-(HCl_4Cat)(Cl_4Cat) were obtained as 2-propanol solvates from a reaction in which KOH and the PPh_4^+ cation were combined prior to addition of protonated catechol. These crystals are triclinic, space group $P\bar{1}$, and form in a unit cell of dimensions $a =$ 12.371 (2) Å, $b = 14.211$ (3) Å, $c = 20.946$ (4), $\alpha = 82.05$ (2)°, $\beta = 79.30$ (2)°, $\gamma = 64.45$ (2)°, and $V = 3258$ (1) Å^3 with R = 0.049 and $R_w = 0.058$. The complex contains a singly protonated Cl_4Cat ligand that is coordinated with the metal through one oxygen atom and hydrogen bonded to the oxygen of the adjacent Cl_4Cat ligand through the protonated oxygen. Carbon-oxygen bond lengths to the coordinated catecholate oxygens are 1.324 (12) Å for the chelated ligand and 1.314 (14) Å to the coordinated oxygen of HCl_4Cat. The anomalously short C-O lengths of the two complexes may arise from a strong ligand-to-metal charge-transfer interaction for the tetrachlorocatecholate ligands. This appears further in the form of intense, low-energy charge-transfer transitions in the visible that extend into the near-IR. Bonding in the members of the bis(quinonato)iron redox series is described in terms of a molecular orbital diagram originally calculated for members of the related chromium series. A feature of interest in this analysis is that while the catecholate π-levels of Fe(bpy)(Cat)$_2^-$ lie lower in energy than the metal 3d levels, they are the sites of redox activity through the series.

Introduction

Much of the bioinorganic chemistry of catechols has concerned complexes of iron. Enterobactin, a siderophore produced by enteric bacteria, forms a tris catecholate chelate with ferric iron.[4] Ferric complexes containing a single chelated catecholate ligand appear as intermediates during the function of the dioxygenase enzymes that catalyze catechol oxidation to carboxylic acids.[5] Studies on proteins that have high DOPA functionality have indicated the presence of chelated iron(III)-catecholate species.[6] With the high affinity of Fe(III) for catecholate ligands and the ubiquity of proteins containing catechol functionalities, it is likely that the bioinorganic interest in Fe(III)-catecholate species will continue to grow.

Model studies on simple iron-catecholate complexes have provided important spectroscopic probes for use in the characterization of more complex biological systems. This has been particularly true for the tris(catecholato)iron(III) complexes and their relationship with the iron complexes of catechol siderophores.[7] Studies by Que on simple LFe(Cat) complexes containing tripodal tetradentate counter ligands have provided insights into the form and function of the intradiol catechol dioxygenase enzymes.[8] The mechanism of the $FeCl_3$/pyridine catechol oxidation system studied by Funabiki may involve a related Fe(Cat) intermediate.[9]

Much less attention has been devoted to the bis(catecholato)iron complexes. Spectroscopic titrations on Fe^{3+}-Cat solutions have indicated that a transition at 570 nm is characteristic of the bis(catecholato)iron(III) chromophore, with presumably two water molecules occupying other coordination sites of the octahedron.[10] Structural and spectral characterization on a Fe(acac)(Cat)$_2^{2-}$ species containing a functionalized catecholate ligand has shown that the complex possesses a monomeric structure and that it exhibits a visible absorption at 535 nm.[11] In this report we describe the results of studies carried out on bis(catecholato)iron complexes containing bipyridine as the counter ligand.

Experimental Section

Materials. 2,2'-Bipyridine, triphenylphosphine, 3,5-di-*tert*-butyl-1,2-benzoquinone, and cobaltocene were purchased from Aldrich. Iron

(1) University of Colorado.
(2) Visiting Scholar from Wuhan University, P.R. China.
(3) University of California at San Diego.
(4) (a) Matzanke, B. F.; Muller-Matzanke, G.; Raymond, K. N. In *Iron Carriers and Iron Proteins*; Loehr, T. M., Ed.; VCH Publishers: New York, 1989; p 1. (b) *Iron Transport in Microbes, Plants and Animals*; Winlelmann, G., van der Helm, D., Neilands, J. B., Eds.; VCH Publishers: New York, 1987. (c) Raymond, K. N.; Muller, G.; Matzanke, B. F. *Topics in Current Chemistry*; Boschke, F. L., Ed.; Springer-Verlag: Berlin, 1984; Vol. 123, pp 50-102. (d) Neilands, J. B. *Annu. Rev. Microbiol.* **1982**, *36*, 285.
(5) Que, L., Jr. In *Iron Carriers and Iron Proteins*; Loehr, T. M., Ed.; VCH Publishers: New York, 1989; p 467.
(6) (a) Dorsett, L. C.; Hawkins, C. J.; Grice, J. A.; Lavin, M. F.; Merefield, P. M.; Parry, D. L.; Ross, I. L. *Biochemistry* **1987**, *26*, 8078. (b) Waite, J. H. *J. Comp. Physiol. B* **1986**, *156*, 491.
(7) (a) Ecker, D. J.; Loomis, L. D.; Cass, M. E.; Raymond, K. N. *J. Am. Chem. Soc.* **1988**, *110*, 2457. (b) Avdeef, A.; Sofen, S. R.; Bregante, T. L.; Raymond, K. N. *J. Am. Chem. Soc.* **1978**, *100*, 5362. (c) Hider, R. C.; Mohd-Nor, A. R.; Silver, J.; Morrison, I. E. G.; Rees, L. V. C. *J. Chem. Soc., Dalton Trans.* **1981**, 609. (d) Anderson, B. F.; Buckingham, D. A.; Robertson, G. B.; Webb, J.; Murray, K. S.; Clark, P. E. *Nature* **1976**, *262*, 722.
(8) Cox, D. D.; Que, L., Jr. *J. Am. Chem. Soc.* **1988**, *110*, 8085.
(9) (a) Funabiki, T.; Tsujimoto, M.; Ozawa, S.; Yoshida, S. *Chem. Lett.* **1989**, 1267. (b) Funabiki, T.; Mizoguchi, A.; Sugimoto, T.; Tada, S.; Tsuji, M.; Sakamoto, H.; Yoshida, S. *J. Am. Chem. Soc.* **1986**, *108*, 2921.
(10) Harris, W. R.; Carrano, C. J.; Cooper, S. R.; Sofen, S. R.; Avdeef, A.; McArdle, J. V.; Raymond, K. N. *J. Am. Chem. Soc.* **1979**, *101*, 6097.
(11) Buckingham, D. A.; Clark, C. R.; Weller, M. G.; Gainsford, G. J. *J. Chem. Soc., Chem. Commun.* **1982**, 779.

0020-1669/92/1331-0870$03.00/0

pentacarbonyl and anhydrous ferric chloride were purchased from Strem. All reagents were used as received. Tetrachlorocatechol[12] and Fe(Cl$_4$SQ)$_3$[13] were prepared by published procedures.

Preparation of Complexes. Fe(bpy)(Cl$_4$SQ)(Cl$_4$Cat). Degassed toluene (40 mL) was added to a mixture of Fe(Cl$_4$SQ)$_3$ (0.80 g, 1.0 mmol) and 2,2′-bipyridine (0.23 g, 1.5 mmol). The solution was stirred for 12 h, reduced to approximately 20 mL in volume, chilled, and filtered. Fe(bpy)(Cl$_4$SQ)(Cl$_4$Cat) was obtained as a dark blue powder. Material isolated from the reaction was recrystallized from THF and dried thoroughly. Anal. Calcd for $C_{22}H_8O_4N_2Cl_8Fe$: C, 37.55; H, 1.15; N, 3.98; Fe, 7.94. Found: C, 37.43; H, 1.69; N, 3.54; Fe, 7.67.

(PPh$_4$)[Fe(bpy)(Cl$_4$Cat)$_2$]. An ethanol solution (50 mL) containing $FeCl_3$ (0.16 g, 1.0 mmol) and tetrachlorocatechol (0.50 g, 2.0 mmol) was treated first with an ethanol solution (20 mL) containing 0.23 g of KOH, followed by a second ethanol solution (10 mL) containing (0.16 g, 1.0 mmol) of 2,2′-bipyridine. The resulting dark blue solution was stirred at room temperature under N_2 for 2 h. A third ethanol solution (20 mL) containing PPh_4Br (0.42 g, 1.0 mmol) was then added, the mixture was stirred for an additional 1 h, and the volume of the solution was reduced to approximately 20 mL. The product was separated from solution by filtration and recrystallized from a CH_2Cl_2/EtOH solution to give 0.86 g of (PPh$_4$)[Fe(bpy)(Cl$_4$Cat)$_2$]·CH_2Cl_2 in 76% yield.

(CoCp$_2$)[Fe(bpy)(Cl$_4$Cat)$_2$]. A toluene solution (25 mL) containing Fe(bpy)(Cl$_4$SQ)(Cl$_4$Cat) (0.71 g, 1.0 mmol) was treated with a toluene solution containing $CoCp_2$ (0.16 g, 1.0 mmol). The product (CoCp$_2$)[Fe(bpy)(Cl$_4$Cat)$_2$] was filtered from solution as a blue precipitate and recrystallized from CH_2Cl_2. Spectroscopic and electrochemical characterization indicated that the anion of the complex was of the same form as the anion obtained using the procedure above.

Fe(OPPh$_3$)$_3$(Cl$_4$CatH)(Cl$_4$Cat). The complex was isolated in low yield from a synthetic procedure similar to the reaction described above for (PPh$_4$)[Fe(bpy)(Cl$_4$Cat)$_2$] but intended to give (PPh$_4$)[Fe(py)$_2$(Cl$_4$Cat)$_2$]. Pyridine was substituted for bipyridine in the procedure, and the KOH and PPh_4Br solutions were added prior to addition of tetrachlorocatechol. Apparently the PPh_4^+ cation reacted with OH^- to give $OPPh_3$ and benzene. Approximately 75 mg of the neutral complex was isolated from the reaction and recrystallized from a CH_2Cl_2/2-propanol solution. Crystals were obtained as 2-propanol solvates, Fe(OPPh$_3$)$_3$(Cl$_4$CatH)(Cl$_4$Cat)·C_3H_7OH.

Physical Measurements. Electronic spectra were recorded on a Perkin-Elmer Lambda 9 spectrophotometer. Infrared spectra were obtained on an IBM IR/30 FTIR spectrometer with samples prepared as KBr pellets. ^1H NMR spectra were recorded on a Varian VXR 300S spectrometer. Cyclic voltammograms were obtained with a Cypress CYSY-1 computer-controlled electroanalysis system in CH_2Cl_2 solutions. A platinum disk working electrode and a platinum wire counter electrode were used. A Ag/Ag$^+$ reference electrode was used that consisted of a CH_3CN solution of $AgPF_6$ in contact with a silver wire placed in glass tubing with a Vycor frit at one end to allow ion transport. Tetrabutylammonium perchlorate (TBAP) was used as the supporting electrolyte, and the ferrocene/ferrocenium couple was used as an internal standard.

Magnetic susceptibility data were collected using a VTS Model 900 SQUID magnetometer (BTi, Inc., San Diego, CA) in an applied field of 10.00 kG. Temperature control was achieved using a BTi digital temperature control device. Data were corrected for residual diamagnetism using Pascal's constants.[14] ^{57}Fe Mossbauer spectra were collected in the constant-acceleration mode using a vertical-drive spectrometer.[15] Isomer shifts are referenced to iron foil at 300 K but are not corrected for the second-order Doppler shift. Data were fit to Lorentzian line shapes using a modified version of a previously reported computer program.[16]

Crystallographic Structure Determinations. (PPh$_4$)[Fe(bpy)(Cl$_4$Cat)$_2$]. Dark blue prismatic crystals of (PPh$_4$)[Fe(bpy)(Cl$_4$Cat)$_2$]·CH_2Cl_2 were obtained by slow evaporation of a CH_2Cl_2/ethanol solution of the complex. Axial photographs indicated triclinic symmetry, and the centered settings of 25 reflections in the 2θ range between 18–28° gave the unit cell dimensions listed in Table I. Data were collected by θ–2θ scans within the angular range 3.0–50.0°. The structure was solved by direct methods. Final cycles of least-squares refinement converged with discrepancy indices of $R = 0.062$ and $R_w = 0.074$. Final positional parameters for selected atoms of the structure are contained in Table II. Tables containing full listings of atom positions, anisotropic thermal parameters, and hydrogen atom locations are available as supplementary material.

Fe(OPPh$_3$)$_3$(HCl$_4$Cat)(Cl$_4$Cat). Dark blue crystals of Fe(OPPh$_3$)$_3$(HCl$_4$Cat)(Cl$_4$Cat)·C_3H_7OH were obtained by slow evaporation of a CH_2Cl_2/2-propanol solution of the complex. Axial photographs indicated

Table I. Crystallographic Data for (PPh$_4$)[Fe(bpy)(Cl$_4$Cat)$_2$]·CH_2Cl_2 and Fe(OPPh$_3$)$_3$(Cl$_4$CatH)(Cl$_4$Cat)·C_3H_7OH

	(PPh$_4$)-[Fe(bpy)(Cl$_4$Cat)$_2$]	Fe(OPPh$_3$)$_3$-(Cl$_4$CatH)(Cl$_4$Cat)
mol wt	1128.1	1441.5
color	blue	blue
cryst system	triclinic	triclinic
space group	$P\bar{1}$	$P\bar{1}$
a, Å	9.633 (2)	12.371 (2)
b, Å	13.868 (3)	14.211 (3)
c, Å	19.543 (3)	20.946 (4)
α, deg	70.99 (2)	82.05 (2)
β, deg	89.11 (2)	79.30 (2)
γ, deg	79.78 (2)	64.45 (2)
V, Å^3	2426.7 (9)	3257.5 (11)
Z	2	2
D_{calcd}, g cm^{-3}	1.544	1.470
D_{exptl}, g cm^{-3}	1.52	1.50
μ, cm^{-1} [a]	9.43	6.88
T_{max}, T_{min}	0.964, 0.687	0.926, 0.908
R, R_w	0.062, 0.074	0.049, 0.058
GOF	1.67	1.12

[a] Radiation, Mo Kα (0.710 73 Å); temp, 294–297 K.

Table II. Selected Atom Coordinates for the Fe(bpy)(Cl$_4$Cat)$_2^-$ Anion

	x/a	y/b	z/c
Fe	2007 (1)	709 (1)	1403 (1)
O1	3359 (5)	1687 (3)	1109 (3)
O2	1273 (5)	1611 (3)	1977 (2)
C1	3089 (7)	2446 (5)	1393 (4)
C2	1948 (7)	2400 (5)	1866 (3)
C3	1595 (8)	3176 (6)	2175 (4)
C4	2365 (8)	3988 (5)	2033 (4)
C5	3499 (8)	4016 (5)	1585 (4)
C6	3859 (7)	3228 (5)	1286 (4)
Cl1	199 (3)	3127 (2)	2738 (1)
Cl2	1878 (3)	4954 (2)	2418 (1)
Cl3	4437 (3)	5005 (2)	1410 (1)
Cl4	5290 (2)	3233 (2)	732 (1)
O3	701 (5)	−295 (4)	1831 (2)
O4	3399 (5)	−438 (3)	2040 (2)
C7	1383 (7)	−1158 (6)	2288 (4)
C8	2863 (7)	−1263 (6)	2393 (4)
C9	3638 (7)	−2174 (6)	2844 (4)
C10	2986 (8)	−2985 (5)	3253 (4)
C11	1539 (9)	−2879 (5)	3172 (4)
C12	749 (7)	−1997 (5)	2689 (4)
C15	5449 (2)	−2258 (2)	2915 (1)
C16	3978 (3)	−4095 (2)	3840 (1)
C17	697 (2)	−3852 (2)	3714 (1)
C18	−1080 (2)	−1856 (2)	2592 (1)
N1	2621 (6)	93 (4)	525 (3)
N2	471 (6)	1559 (4)	510 (3)
C13	3732 (8)	−650 (6)	570 (4)
C14	4077 (9)	−1058 (6)	17 (5)
C15	3204 (10)	−694 (7)	−589 (5)
C16	2047 (9)	65 (6)	−660 (4)
C17	1786 (8)	459 (5)	−84 (4)
C18	613 (7)	1293 (6)	−104 (4)
C19	−318 (9)	1817 (7)	−698 (4)
C20	−1352 (9)	2621 (7)	−674 (5)
C21	−1483 (9)	2915 (7)	−65 (5)
C22	−545 (8)	2340 (6)	533 (5)

(12) (a) Jackson, L. C.; MacLaurin, R. D. *J. Am. Chem. Soc.* **1907**, *37*, 11. (b) Abbreviations: BQ, SQ, and Cat have been used to refer to benzoquinone, semiquinone, and catecholate forms of the quinone ligands, Q has been used to refer to quinone ligands of unspecified charge, and DB and Cl$_4$ have been used as prefixes for the 3,5-di-*tert*-butyl- and tetrachloro-substituted quinone ligands.
(13) Buchanan, R. M.; Kessel, S. L.; Downs, H. H.; Pierpont, C. G.; Hendrickson, D. N. *J. Am. Chem. Soc.* **1978**, *100*, 7894.
(14) *Theory and Applications of Molecular Paramagnetism*; Boudreaux, E. A., Mulay, L. N., Eds.; John Wiley: New York, 1976.
(15) Cohn, M. J.; Timken, M. D.; Hendrickson, D. N. *J. Am. Chem. Soc.* **1984**, *106*, 6683.
(16) Chrisman, B. L.; Tumolillo, T. A. *Comput. Phys. Commun.* **1971**, *2*, 322.

Table III. Selected Atom Coordinates for $Fe(OPPh_3)_3(HCl_4Cat)(Cl_4Cat)$

	x/a	y/b	z/c
Fe	839 (1)	1765 (1)	2536 (1)
Cl1	574 (3)	1228 (3)	279 (2)
Cl2	-1943 (3)	2804 (3)	-154 (2)
Cl3	-3943 (3)	4270 (3)	858 (2)
Cl4	-3439 (2)	4121 (3)	2298 (2)
O1	-910 (5)	2635 (5)	2481 (3)
O2	759 (6)	1471 (5)	1641 (3)
C1	-1203 (9)	2708 (8)	1893 (5)
C2	-294 (9)	2065 (8)	1436 (5)
C3	-537 (10)	2086 (8)	813 (5)
C4	-1661 (12)	2761 (10)	630 (6)
C5	-2558 (10)	3413 (9)	1085 (7)
C6	-2335 (9)	3362 (8)	1719 (6)
Cl5	2711 (3)	2028 (3)	3950 (2)
Cl6	2441 (3)	4072 (3)	4495 (2)
Cl7	178 (4)	6147 (3)	4273 (2)
Cl8	-1869 (4)	6113 (3)	3613 (2)
O3	612 (5)	2243 (5)	3385 (3)
O4	-1486 (7)	4096 (7)	3298 (4)
C7	-514 (11)	4062 (9)	3537 (5)
C8	520 (9)	3117 (9)	3582 (5)
C9	1433 (10)	3152 (10)	3874 (6)
C10	1343 (12)	4067 (13)	4098 (6)
C11	329 (15)	4974 (12)	4019 (6)
C12	-599 (11)	4982 (9)	3732 (6)
P1	-306 (2)	-13 (2)	3191 (1)
O5	565 (5)	476 (5)	2943 (3)
P2	3832 (2)	-59 (2)	2388 (2)
O6	2647 (5)	862 (5)	2432 (3)
P3	1530 (3)	3792 (2)	1685 (2)
O7	1229 (6)	3009 (5)	2141 (3)
H1	-1277 (74)	3502 (70)	3141 (44)

triclinic symmetry, and the centered settings of 25 reflections in the 2θ range 18–25° gave the unit cell dimensions listed in Table I. Data were collected by θ–2θ scans within the angular range 3.0–45.0°. The structure was solved by direct methods. The 2-propanol solvate molecule was found to be located near the inversion center at [$^1/_2$, $^1/_2$, $^1/_2$] and disordered. Atom locations were refined with fractional occupancy factors. Final cycles of least-squares refinement converged with discrepancy indices of $R = 0.049$ and $R_w = 0.058$. Final positional parameters for selected atoms of the structure are contained in Table III. Tables containing full listings of atom positions, anisotropic thermal parameters, and hydrogen atom locations are available as supplementary material.

Experimental Results

Synthetic Procedures. Two synthetic routes are available to the $Fe(bpy)(Cat)_2^-$ anions. The most straightforward involves the addition of the protonated catechol, hydroxide base, and bipyridine to a solution containing $FeCl_3$. In preliminary studies, complexes prepared with alkyl-substituted catechol ligands or catechol ligands that have negative oxidation potentials were found to be extremely air sensitive, perhaps through chemistry associated with the Funabiki oxidation system.[9] Since the metal, as Fe(III), is unlikely to be the site of greatest nucleophilicity, the tetrachlorocatecholate ligand was used due to its more positive oxidation potential. This procedure has produced the air-stable $Fe(bpy)(Cl_4Cat)_2^-$ anion, isolated as the PPh_4^+ salt using the procedure described in the Experimental Section. The second approach has involved the synthesis of Fe(bpy)(SQ)(Cat) by treating the parent $Fe(SQ)_3$ complex with bipyridine. Reduction of Fe(bpy)(SQ)(Cat), by either chemical or electrochemical means, occurs at the semiquinone ligand and may be used to form the $Fe(bpy)(Cat)_2^-$ anion. This procedure has been carried out using cobaltocene as a chemical reductant and has been used to synthesize $[Co(Cp)_2][Fe(bpy)(Cl_4Cat)_2]$ from $Fe(bpy)(Cl_4SQ)(Cl_4Cat)$. A similar reaction was carried out using Fe(bpy)(DBSQ)(DBCat).[17] The addition of cobaltocene to this complex under a nitrogen environment in toluene solution led to formation of platelike crystals of a complex that was extraordinarily air sensitive. Even trace quantities of oxygen led to rapid decomposition of the complex as a solid. Electrochemical characterization on Fe(bpy)(DBSQ)(DBCat) showed irreversible reduction of the DBSQ ligand at −0.416 V (vs Fc/Fc^+), a potential that is approximately 0.5 V more negative than the corresponding reduction of $Fe(bpy)(Cl_4SQ)(Cl_4Cat)$. While the form of Fe(bpy)(DBSQ)(DBCat) is unclear,[17] magnetic characterization suggests that it may be oligomeric similar to the [Fe(DBSQ)(DBCat)]$_4$ tetramer.[18] The potential of the reduction process is not inconsistent with what might be expected for the reduction of a coordinated DBSQ ligand of Fe(bpy)(DBSQ)(DBCat). These results appear to confirm the view that the difference in oxygen sensitivity between the reduced Cl_4Cat complex and the DBCat complex is related to the relative oxidation potentials of the different catecholate ligands.

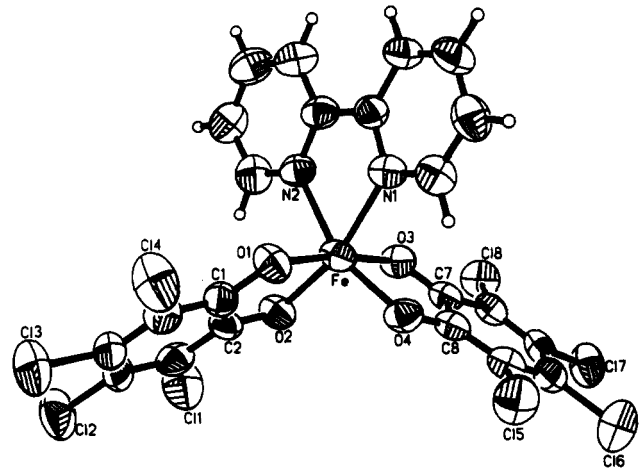

Figure 1. View of the $Fe(bpy)(Cl_4Cat)_2^-$ anion.

Interests in investigating the three-membered redox series $Fe(bpy)(SQ)_2^+$–$Fe(bpy)(SQ)(Cat)$–$Fe(bpy)(Cat)_2^-$, which we had described earlier for Cr,[19] led us to investigate the oxidation of Fe(bpy)(DBSQ)(DBCat). The alkyl-substituted quinone ligands of this complex would favor a stable oxidation product, and the related tetrachloroquinone complex was judged to be too strong an oxidant in its cationic form. Treatment of Fe(bpy)(DBSQ)(DBCat) with $AgPF_6$ produced silver metal as a product of oxidation by silver ion, but the complex products obtained were $Fe(DBSQ)_3$ and $Fe(bpy)_3^{2+}$. Questions concerning the form of Fe(bpy)(DBSQ)(DBCat) complicate interpretation of these results, but oxidation appears to be accompanied by disproportionation of a putative $Fe(bpy)(DBSQ)_2^+$ product to give $Fe(DBSQ)_3$ and $Fe(bpy)_3^{3+}$, which, as a strong oxidant, is ultimately reduced to the Fe(II) species. Addition of excess bipyridine to $Fe(bpy)(Cl_4Cat)_2^-$ has been observed to also produce $Fe(bpy)_3^{2+}$ by initial formation of $Fe(bpy)_3^{3+}$. Consequently, only two members of this redox series have been characterized.

The sequence of reagent addition in the first procedure is critical. A reaction carried out by adding base to a solution containing $FeCl_3$ and PPh_4^+ before the addition of H_2Cl_4Cat and bipyridine gave $Fe(OPPh_3)_3(HCl_4Cat)(Cl_4Cat)$. Hydroxide apparently reacts with PPh_4^+ to give triphenylphosphine oxide and benzene. Optical spectra recorded on the complex show broad transitions in the visible at 438 (4800 M^{-1} cm^{-1}) nm and at 584 (5400) nm. Since this complex is of interest as a rare example of a coordinated protonated catechol,[20] its characterization has been included in this report.

Structural Characterization on $(PPh_4)[Fe(bpy)(Cl_4Cat)_2]$. Large plate-shaped crystals of $(PPh_4)[Fe(bpy)(Cl_4Cat)_2]$ were formed by slow evaporation of a dichloromethane solution of the complex.

(17) Lynch, M. W.; Valentine, M.; Hendrickson, D. N. *J. Am. Chem. Soc.* **1982**, *104*, 6982.
(18) Boone, S. R.; Purser, G. H.; Chang, H.-R.; Lowery, M. D.; Hendrickson, D. N.; Pierpont, C. G. *J. Am. Chem. Soc.* **1989**, *111*, 2292.
(19) Buchanan, R. M.; Claflin, J.; Pierpont, C. G. *Inorg. Chem.* **1983**, *22*, 2552.
(20) Heistand, R. H.; Roe, A. L.; Que, L., Jr. *Inorg. Chem.* **1982**, *21*, 676.

Table IV. Selected Bond Lengths and Angles for the $Fe(bpy)(Cl_4Cat)_2^-$ Anion

Bond Lengths (Å)			
Fe–N1	2.183 (7)	Fe–N2	2.178 (5)
Fe–O4	1.971 (4)	Fe–O3	2.013 (5)
Fe–O1	1.991 (5)	Fe–O2	1.975 (5)
N1–C13	1.329 (9)	N1–C17	1.347 (9)
N2–C18	1.362 (10)	N2–C22	1.337 (10)
C13–C14	1.385 (14)	C14–C15	1.362 (12)
C15–C16	1.365 (12)	C16–C17	1.403 (12)
C17–C18	1.457 (10)	C18–C19	1.390 (10)
C19–C20	1.369 (12)	C20–C21	1.377 (15)
C21–C22	1.410 (11)	O4–C8	1.318 (8)
O3–C7	1.306 (7)	C8–C7	1.418 (10)
C8–C9	1.375 (9)	C7–C12	1.409 (10)
C12–C11	1.380 (9)	C12–Cl8	1.745 (7)
C11–C10	1.382 (12)	C11–Cl7	1.741 (8)
C10–C9	1.396 (10)	C10–Cl6	1.720 (6)
C9–C15	1.732 (7)	O1–C1	1.327 (8)
O2–C2	1.327 (8)	C1–C2	1.421 (10)
C1–C6	1.379 (11)	C2–C3	1.388 (11)
C3–C4	1.407 (11)	C3–Cl1	1.721 (8)
C4–C5	1.388 (11)	C4–Cl2	1.733 (8)
C5–C6	1.389 (12)	C5–Cl3	1.715 (8)
C6–Cl4	1.739 (7)		
Bond Angles (deg)			
N1–Fe–N2	74.0 (2)	N1–Fe–O4	87.8 (2)
N2–Fe–O4	159.3 (2)	N1–Fe–O3	94.7 (2)
N2–Fe–O3	90.1 (2)	O4–Fe–O3	81.5 (2)
N1–Fe–O1	91.3 (2)	N2–Fe–O1	95.6 (2)
O4–Fe–O1	94.5 (2)	O3–Fe–O1	172.7 (2)
N1–Fe–O2	164.6 (2)	N2–Fe–O2	92.7 (2)
O4–Fe–O2	106.5 (2)	O3–Fe–O2	93.1 (2)
O1–Fe–O2	82.1 (2)		

Crystals formed by this procedure were found to contain one molecule of dichloromethane per formula unit of complex. The plates appeared "smoky pink" in color when viewed through their thin faces but were dark blue when ground to form a powder. This view is down the crystallographic *a* axis, corresponding to a molecular orientation which is slightly off the pseudo-3-fold axis of the octahedral complex anion. A view of packing in the unit cell corresponding to this orientation is given with the supplementary material. Values for selected bond lengths and angles are given in Table IV, and a view of the complex anion is shown in Figure 1. The Fe–N and Fe–O lengths agree well with values expected for high-spin Fe(III). Carbon–oxygen lengths of the quinone ligands have been found in other structures to be particularly sensitive to charge distribution within the complex. A list of values obtained for semiquinone and catecholate complexes of iron(III) is given in Table V. Semiquinone ligands generally have C–O lengths that are close to 1.28 Å, while chelated catechol lengths are in the 1.34–1.35-Å range. Bridging ligands of both types generally have C–O lengths that are slightly longer than these normal values as is apparent in the structure of the $[Fe(DBSQ)(DBCat)]_4$ tetramer.[18] In this molecule semiquinone and catecholate ligands were clearly distinguishable from their structural differences. No tetrachlorosemiquinone or other tetrachlorocatecholate structures have been reported as complexes of iron, but the structural features of complexes containing other metals indicate that the trend that is apparent in Table V should be expected for the chloronated quinone ligands as well.[25] Intermediate values for C–O lengths have been found for $Ru(DBQ)_3$,

Table V. Carbon–Oxygen Bond Lengths for Iron Catecholate and Semiquinone Complexes

complex	C–O, Å
Catecholates	
$Fe(Cat)_3^{3-}$	1.349 (3)[a]
	1.340 (4)[b]
$Fe(TRENCAM)^{3-}$	1.333 (3)[c]
$Fe(NTA)(DBCat)^{2-}$	1.340 (5)[d]
Fe(BPG)(DBCat)	1.356 (3)[e]
$Fe_4(DBSQ)_4(DBCat)_4$	1.345 (6)[f]
	1.383 (5)[g]
$Fe(bpy)(Cl_4Cat)_2^-$	1.320 (8)[i]
$Fe(OPPh_3)_3(Cl_4CatH)(Cl_4Cat)$	1.32 (1)[i]
Semiquinones	
$Fe(DBSQ)_3$	1.281 (3)[f]
$Fe(PhenSQ)_3$	1.283 (3)[h]
$Fe_4(DBSQ)_4(DBCat)_4$	1.273 (7)[f]
	1.305 (6)[g]

[a] Reference 21. [b] Reference 22. [c] Reference 23. [d] Reference 24. [e] Reference 8. [f] Reference 18. [g] Bridging oxygen atom. [h] Reference 13. [i] This work.

$Ru(t\text{-}Bupy)_2(DBSQ)(DBCat)$, and $Ru(bpy)(SQ)(Cat)$.[26-29] All three complexes have average lengths of 1.32 Å that appear to arise from the effects of intramolecular charge delocalization. Average C–O lengths for the two catecholate ligands of $(PPh_4)[Fe(bpy)(Cl_4Cat)_2]$ are 1.327 (8) Å for the ligand containing O1 and O2 and 1.312 (8) Å for the ligand containing O3 and O4. Both sets of lengths are shorter than typical catecholate values and longer than semiquinone values but average to the 1.32-Å value found for the ruthenium complexes. This result may be viewed as an anomaly of the structure determination or as a feature resulting from a unusual electronic structure related to the chloro substituents of the ligand. However, several structure determinations have been carried out on complexes containing tetrachlorocatecholate and tetrachlorosemiquinone ligands, and average values for the C–O lengths conform to the pattern noted for catecholate and semiquinone complexes containing other quinone ligands. Tetrachlorocatecholate structures include $Pd(PPh_3)_2(Cl_4Cat)$, 1.342 (10) Å;[30] $Mo_2(Cl_4Cat)_8$, 1.34 (1) Å;[31] $W_2(Cl_4Cat)_8$, 1.350 (7) Å;[32] $Re(Cl_4Cat)_3$, 1.343 (8) Å;[25b] $Os(bpy)(Cl_4Cat)_2$, 1.337 (9) Å;[33] $Rh_2(CO)_2(S)(dpm)_2(Cl_4Cat)$, 1.332 (8) Å;[34] $Pt(DMSO)_2(Cl_4Cat)$, 1.332 (9) Å;[35] and $Mo_2(O\text{-}i\text{-}Pr)_6(Cl_4Cat)_2$, 1.330 (9) Å.[36] Structures containing tetrachlorosemiquinone ligands include $Cr(Cl_4SQ)_3$, 1.280 (8) Å;[37] $NiL(Cl_4BQ)(Cl_4SQ)$, 1.26 (1) Å;[38] and $Ru(PPh_3)_2(Cl_4SQ)_2$, 1.296 (8) Å.[25a] Even though individual values obtained for these complexes and for the complexes contained in Table V often vary over 0.02 Å for a specific structure determination, averaged values are in good agreement with the assigned catecholate or semiquinone charge distribution.

Two structures have been reported to have intermediate values for average C–O length. A value of 1.322 (8) Å was reported for $Rh_2(dpm)_2(CO)(Cl_4Cat)$ where dissimilar metals are linked

(21) Raymond, K. N.; Isied, S. S.; Brown, L. D.; Fronczek, F. R.; Nibert, J. H. *J. Am. Chem. Soc.* **1976**, *98*, 1767.
(22) Anderson, B. F.; Buckingham, D. A.; Robertson, G. B.; Webb, J. *Acta Crystallogr.* **1982**, *B38*, 1927.
(23) McMurry, T. J.; Hosseini, M. W.; Garrett, T. M.; Hahn, F. E.; Reyes, Z. E.; Raymond, K. N. *J. Am. Chem. Soc.* **1987**, *109*, 7196.
(24) Que, L., Jr.; Kolanczyk, R. C.; White, L. S. *J. Am. Chem. Soc.* **1987**, *109*, 5373.
(25) (a) Bhattacharya, S.; Pierpont, C. G. *Inorg. Chem.* **1991**, *30*, 1511. (b) deLearie, L. A.; Haltiwanger, R. C.; Pierpont, C. G. *Inorg. Chem.* **1987**, *26*, 817.
(26) Bhattacharya, S.; Boone, S. R.; Pierpont, C. G. *J. Am. Chem. Soc.* **1990**, *112*, 4561.
(27) Haga, M.; Dodsworth, E. S.; Lever, A. B. P.; Boone, S. R.; Pierpont, C. G. *J. Am. Chem. Soc.* **1986**, *108*, 7321.
(28) Boone, S. R.; Pierpont, C. G. *Inorg. Chem.* **1987**, *26*, 1769.
(29) Boone, S. R.; Pierpont, C. G. *Polyhedron* **1990**, *9*, 2267.
(30) Pierpont, C. G.; Downs, H. H. *Inorg. Chem.* **1975**, *14*, 343.
(31) Pierpont, C. G.; Downs, H. H. *J. Am. Chem. Soc.* **1975**, *97*, 2123.
(32) deLearie, L. A.; Pierpont, C. G. *Inorg. Chem.* **1988**, *27*, 3842.
(33) Bhattacharya, S.; Pierpont, C. G. *Inorg. Chem.*, in press.
(34) Balch, A. L.; Catalano, V. J.; Olmstead, M. M. *Inorg. Chem.* **1990**, *29*, 1638.
(35) Khodashova, T. S.; Porai-Koshits, M. A.; Rudii, R. I.; Cherkashina, N. V.; Moiseev, I. I. *Koord. Khim.* **1984**, *10*, 850.
(36) Blatchford, T. P.; Chisholm, M. H.; Huffman, J. C. *Inorg. Chem.* **1988**, *27*, 2059.
(37) Pierpont, C. G.; Downs, H. H. *J. Am. Chem. Soc.* **1976**, *98*, 4834.
(38) Benelli, C.; Dei, A.; Gatteschi, D.; Pardi, L. *J. Am. Chem. Soc.* **1988**, *110*, 6897.

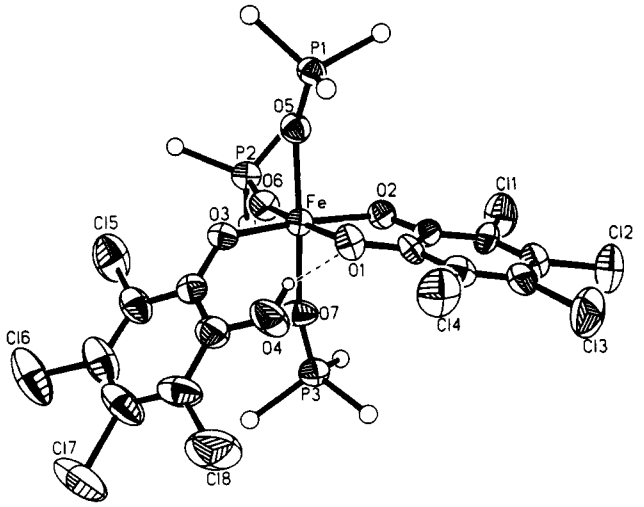

Figure 2. View of $Fe(OPPh_3)_3(HCl_4Cat)(Cl_4Cat)$, showing the hydrogen-bonding interaction between oxygen atoms of the protonated and deprotonated catecholate ligands. Phenyl rings of the $OPPh_3$ ligands have been omitted.

by a dative Rh–Rh bond.[39] The bridging catecholate ligand of $[Cu_2(L)(Cl_4Cat)]^+$ was reported to have an average C–O length of 1.322 (16) Å.[40] The relationship between this complex and catecholate species that form from tyrosine hydroxylation by tyrosinase has been noted. Reductive elimination of the catecholate as benzoquinone has been proposed to restore the enzyme to its reduced state, and contraction of the C–O length in this model complex may be pertinent.

In the context of the structural features of other catecholate and semiquinone complexes, the intermediate value of the C–O lengths of $Fe(bpy)(Cl_4Cat)_2^-$ appears to point to a delocalized $Fe^{II}(SQ)(Cat)^-$ charge distribution for the complex.

Structural Characterization on $Fe(OPPh_3)_3(HCl_4Cat)(Cl_4Cat)$. Dark blue crystals of this complex were obtained as 2-propanol solvates. A view of the inner coordination geometry of the complex is given in Figure 2. Triphenylphosphine oxide ligands are coordinated at meridional sites about the octahedral iron atom. One catecholate ligand is chelated normally to the iron; the second is coordinated to the metal through one oxygen atom. The other oxygen atom of this ligand, O4, contains a proton that is hydrogen bonded with one oxygen atom of the chelated ligand. Selected bond distances and angles for this molecule are given in Table VI. Two of the triphenylphosphine oxide ligands have Fe–O–P angles that are in the 163° range found for the $[Mn(OPPh_3)(Br_4Cat)_2]_2^{2-}$ dianion;[41] the third containing O5 is more sharply bent with an angle of 148.4 (4)°. Iron–oxygen lengths are slightly longer to the trans triphenylphosphine oxide ligands than to the ligand containing O6 which is trans to the catecholate oxygen O1. Iron–oxygen lengths of the chelated catecholate ligand are comparable with Fe–O lengths of the $Fe(bpy)(Cl_4Cat)_2^-$ anion. The length to O3 is somewhat shorter than these values but comparable to lengths reported for terminal phenolate ligands coordinated to Fe(III).[42] Structural features of the two catecholate ligands are of specific interest with respect to questions concerning charge distribution raised by the C–O lengths of $Fe(bpy)(Cl_4Cat)_2^-$. Carbon–oxygen lengths of the chelated ligand are 1.324 (12) and 1.325 (12) Å, while the C8–O3 length of the second ligand is 1.314 (14) Å. For comparison, the C–O length to the uncoordinated protonated oxygen is a normal single-bond value of 1.366 (16) Å.

In essence, the pattern of unusually short catecholate C–O bond lengths found for $Fe(bpy)(Cl_4Cat)_2^-$ is carried over to the chelated catecholate ligand of $Fe(OPPh_3)_3(HCl_4Cat)(Cl_4Cat)$.

Physical Properties of $Fe(bpy)(Cl_4SQ)(Cl_4Cat)$. Mossbauer spectra recorded on $Fe(bpy)(Cl_4SQ)(Cl_4Cat)$ at temperatures of 300, 200, and 134 K are similar. Spectra are shown in Figure 3, and parameters obtained from the spectra are listed in Table VII. The 134 K spectrum shows quadrupolar splitting and isomer shift parameters of 0.909 (3) and 0.492 (1) mm/s, respectively. These values are indicative of high-spin ferric iron and are consistent with the mixed-charge ligand formulation for the complex.

The magnetic susceptibility of a powdered sample of $Fe(bpy)(Cl_4SQ)(Cl_4Cat)$ was measured in the 9.39–300 K range; the data plotted as effective moments are given in Figure 4. The effective moment for the compound is roughly independent of temperature between 100 and 300 K with $\mu_{eff} = 5.40$ (5) μ_B. Below 100 K the moment rises slightly and then increases sharply below 20 K to 6.15 μ_B by 9.39 K. For a high-spin Fe(III) complex with a single semiquinone ligand, intramolecular magnetic exchange will produce two states with $S = 2$ and $S = 3$; when the exchange is antiferromagnetic, the $S = 2$ state becomes the ground state.

Table VI. Selected Bond Lengths and Angles for $Fe(OPPh_3)_3(HCl_4Cat)(Cl_4Cat)$

Bond Lengths (Å)			
Fe–O1	1.993 (6)	Fe–O2	2.007 (7)
Fe–O3	1.919 (7)	Fe–O5	2.048 (8)
Fe–O6	2.029 (5)	Fe–O7	2.055 (8)
Cl1–C3	1.728 (10)	Cl2–C4	1.727 (14)
Cl3–C5	1.729 (11)	Cl4–C6	1.725 (10)
O1–C1	1.325 (12)	O2–C2	1.324 (12)
C1–C2	1.405 (13)	C2–C3	1.386 (17)
C4–C3	1.395 (16)	C4–C5	1.402 (16)
C6–C1	1.390 (14)	C6–C5	1.390 (20)
Cl5–C9	1.709 (10)	Cl6–C10	1.723 (18)
Cl7–C11	1.744 (19)	Cl8–C12	1.723 (11)
O3–C8	1.314 (14)	O4–C7	1.366 (16)
C7–C8	1.406 (14)	C8–C9	1.402 (19)
C9–C10	1.395 (24)	C11–C10	1.373 (18)
C11–C12	1.386 (25)	C12–C7	1.379 (20)
P1–O5	1.500 (8)	P2–O6	1.482 (5)
P3–O7	1.490 (8)	O4–H1	0.89 (8)
Bond Angles (deg)			
O1–Fe–O2	80.0 (3)	O1–Fe–O3	89.4 (3)
O2–Fe–O3	169.2 (2)	O1–Fe–O5	93.6 (3)
O2–Fe–O5	91.8 (3)	O3–Fe–O5	90.6 (3)
O1–Fe–O6	170.5 (3)	O2–Fe–O6	90.7 (3)
O3–Fe–O6	99.9 (3)	O5–Fe–O6	88.6 (3)
O1–Fe–O7	90.0 (3)	O2–Fe–O7	89.4 (3)
O3–Fe–O7	88.8 (3)	O5–Fe–O7	176.3 (3)
O6–Fe–O7	87.8 (3)	Fe–O5–P1	148.4 (4)
Fe–O6–P2	162.1 (5)	Fe–O7–P3	164.3 (5)

Table VII. Mossbauer Parameters for $Fe(bpy)(Cl_4SQ)(Cl_4Cat)$ and for the $Fe(bpy)(Cl_4Cat)_2^-$ Anion

T, K	ΔE_Q, mm/s	δ,[a] mm/s	$\Gamma_{1/2}$, mm/s	in area
		$Fe(bpy)(Cl_4SQ)(Cl_4Cat)$		
300	0.881 (6)	0.500 (3)	0.182 (5) 0.213 (6)	−1.446 (16)
200	0.894 (5)	0.497 (2)	0.180 (4) 0.213 (4)	−1.125 (12)
134	0.909 (3)	0.492 (1)	0.215 (2) 0.238 (3)	−0.477 (17)
		$(PPh_4)[Fe(bpy)(Cl_4Cat)_2]\cdot CH_2Cl_2$		
300	0.748 (12)	0.478 (6)	0.233 (11) 0.267 (13)	−2.56 (3)
200	0.784 (15)	0.462 (7)	0.297 (13) 0.340 (16)	−2.32 (2)
132	0.825 (16)	0.446 (8)	0.364 (16) 0.408 (18)	−2.28 (2)

[a] Isomer shift relative to iron foil at room temperature.

(39) Ladd, J. A.; Olmstead, M. M.; Balch, A. L. *Inorg. Chem.* **1984**, *23*, 2318.
(40) Karlin, K. D.; Gultneh, Y.; Nicholson, T.; Zubieta, J. *Inorg. Chem.* **1985**, *24*, 3725.
(41) Larsen, S. K.; Pierpont, C. G.; DeMunno, G.; Dolcetti, G. *Inorg. Chem.* **1986**, *25*, 4828.
(42) (a) Yan, S.; Que, L., Jr.; Taylor, L. F.; Anderson, O. P. *J. Am. Chem. Soc.* **1988**, *110*, 5222. (b) Snyder, B. S.; Patterson, G. S.; Abrahamson, A. J.; Holm, R. H. *J. Am. Chem. Soc.* **1989**, *111*, 5214.
(43) Lever, A. B. P.; Auburn, P. R.; Dodsworth, E. S.; Haga, M.; Liu, W.; Melnik, M.; Nevin, W. A. *J. Am. Chem. Soc.* **1988**, *110*, 8076.

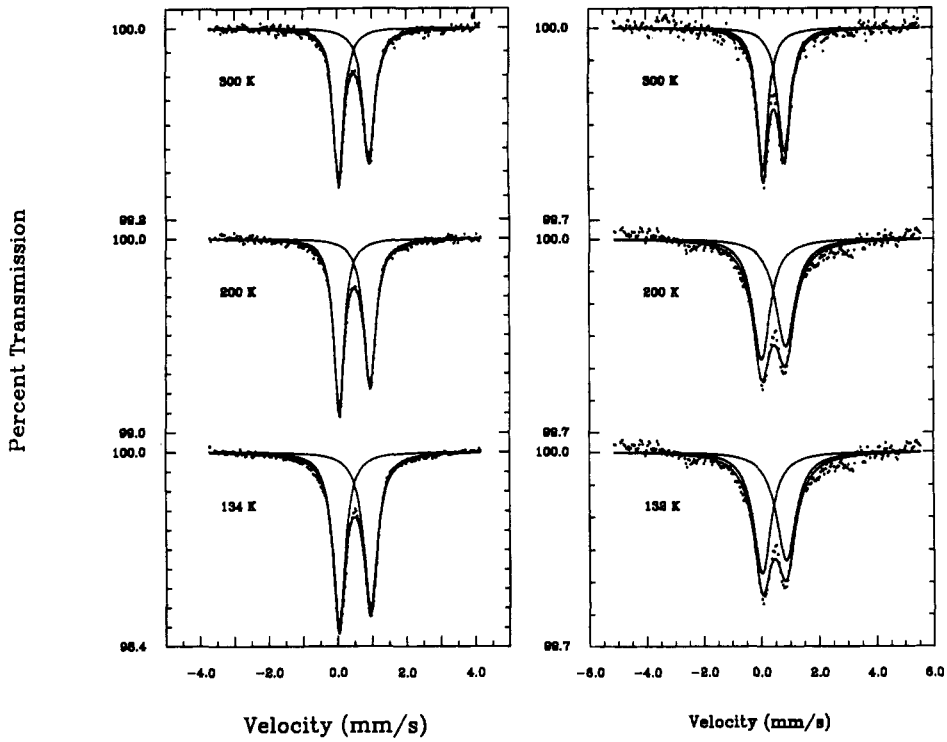

Figure 3. Mossbauer spectra recorded on Fe(bpy)(Cl_4SQ)(Cl_4Cat) (left) and (PPh_4)[Fe(bpy)(Cl_4Cat)$_2$] (right).

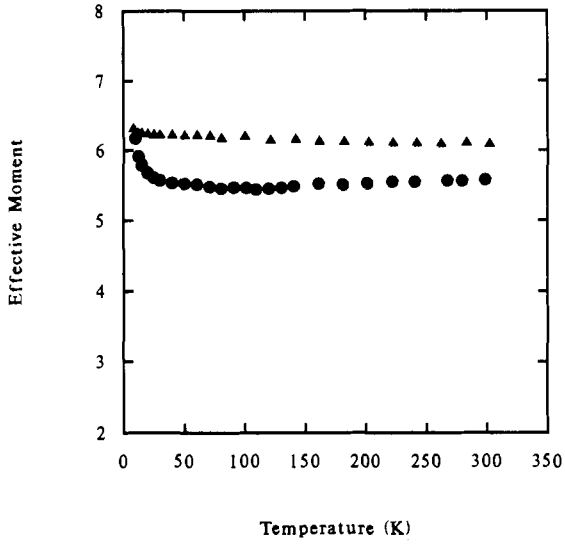

Figure 4. Plots of effective moment versus temperature for (●) Fe(bpy)(Cl_4SQ)(Cl_4Cat) and (▲) (PPh_4)[Fe(bpy)(Cl_4Cat)$_2$] in an applied field of 10.00 kG.

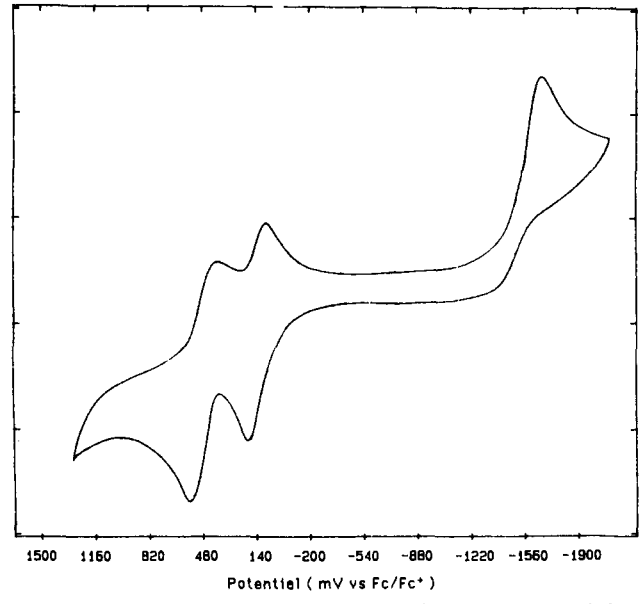

Figure 5. Cyclic voltammogram of Fe(bpy)(Cl_4Cat)$_2^-$ recorded in CH_2Cl_2 at a scan rate of 100 mV/s using TBAP as the supporting electrolyte.

The spin-only value for a $S = 2$ state is 4.89 μ_B, whereas a $S = 3$ state has a spin-only moment of 6.93 μ_B. If both states are thermally populated, i.e., the energy separation is much less than kT, then the spin-only moment of 6.15 μ_B is not unusual. The temperature-independent value of 5.50 μ_B for Fe(bpy)(Cl_4SQ)(Cl_4Cat) is something of an enigma, in that it lies between the values expected for a strongly-coupled system and that of a weakly-coupled system. On the basis of previous observations by Lynch et al.[17] and our belief that the sharp low-temperature rise in the moment is likely due to intermolecular ferromagnetic interactions, we conclude that the magnetic data indicate strong antiferromagnetic coupling between the high-spin ferric center and the semiquinone radical in Fe(bpy)(Cl_4SQ)(Cl_4Cat). Lynch and co-workers reported effective moments for the strongly-coupled system Fe(phen)(DBSQ)(DBCat) of 5.27 μ_B at 245 K, but no explanation for the unusually high $S = 2$ moment was given. Since a high-spin ferric ion is orbitally nondegenerate, a large orbital contribution to the moment is *not* expected. The semiquinone ligand with its unpaired electron in a π^*-orbital will have some orbital degeneracy associated with it, but it is questionable whether this factor will manifest itself in large deviations from the spin-only value. One possible explanation for the high moment is the presence of an excited-state configuration formulated as Fe^{II}(bpy)(Cl_4SQ)$_2$. Configuration interaction between this state and the mixed-ligand ground state could instill some orbital angular momentum into the ground state in much the same way that CI produces field-induced paramagnetism (TIP) in diamagnetic species.

Electrochemical characterization has been carried out on neutral Fe(bpy)(Cl_4SQ)(Cl_4Cat) and on the Fe(bpy)(Cl_4Cat)$_2^-$ anion. The two complexes show redox couples at similar potentials. Oxidation of the two catecholate ligands of the anionic complex occurs in the two steps shown in Figure 5. The first appears at a potential of +0.130 (78) V (Fc/Fc$^+$) to give the neutral mix-

ed-charge ligand complex; the second oxidation occurs at +0.489 (130) V to give the $Fe(bpy)(Cl_4SQ)_2^+$ cation. Reduction of the metal to Fe(II) appears irreversibly for the anionic complex at −1.566 V. The optical spectrum of $Fe(bpy)(Cl_4SQ)(Cl_4Cat)$ in the visible region consists of a sharp unsymmetrical band at 435 nm (4400 M^{-1} cm^{-1}) and a broad, unsymmetrical absorption that has maximum intensity at 625 (4100) nm but tails into the near-IR to slightly beyond 1000 nm. Both bands appear to consist of at least two overlapped transitions.

Physical Properties of $(PPh_4)[Fe(bpy)(Cl_4Cat)_2]$. ^{57}Fe Mossbauer spectra for $(PPh_4)[Fe(bpy)(Cl_4Cat)_2]$ collected between 130 and 300 K are shown in Figure 3. The spectrum at each temperature can be fit to a single quadrupole-split doublet with hyperfine parameters consistent with high-spin Fe(III) (Table VIII); this is in accord with the formulation of the compound as a bis(catecholate) species. One curious aspect of the low-temperature spectrum of the neutral compound $Fe(bpy)(Cl_4SQ)(Cl_4Cat)$ becomes apparent upon examining the spectral line widths observed for $(PPh_4)[Fe(bpy)(Cl_4Cat)_2]$. It can be seen that, although a single quadrupole doublet adequately models the 132 K spectrum for $(PPh_4)[Fe(bpy)(Cl_4Cat)_2]$, the fit is not as good as the fit indicated for $Fe(bpy)(Cl_4SQ)(Cl_4Cat)$ at 134 K. The slight broadening of the spectrum of the anionic complex suggests the inset of a magnetic pattern, a phenomenon quite commonly found for Fe(III) complexes. However, a similar broadening of the 134 K spectrum of $Fe(bpy)(Cl_4SQ)(Cl_4Cat)$ is not evident. This difference is quantified in Table VII; the average half-line widths at room temperature for the neutral and anionic compounds are 0.198 and 0.250 mm/s, respectively, whereas at the lowest temperatures these averages are 0.227 and 0.386 mm/s. Although admittedly a minor point, it does illustrate an interesting effect arising from the magnetic exchange interaction between the ferric ion and semiquinone radical in the mixed-ligand complex which is not present in the bis(catecholate) species.

A plot of effective moment versus temperature for $(PPh_4)[Fe(bpy)(Cl_4Cat)_2]$ is shown in Figure 4. The moment is essentially temperature-independent from 300 to about 20 K at 6.15 (5) μ_B. The moment does rise slightly to 6.31 μ_B by 7.98 K; this is likely the result of weak intermolecular ferromagnetic interactions similar to those found in the neutral complex (vide supra). That the intermolecular interactions appear to be weaker in this complex as compared to $Fe(bpy)(Cl_4SQ)(Cl_4Cat)$ is consistent with the anionic nature of the compound; the presence of the PPh_4^+ cations in the lattice will tend to insulate the anions and attenuate intermolecular magnetic interactions. The observed value for μ_{eff} is somewhat higher than the value of 5.91 μ_B expected for a simple high-spin ferric complex. However, the compound was found to contain one CH_2Cl_2 solvate per formula unit of complex from the crystallographic characterization. Loss of some solvent likely occurred between the time of sample preparation and collection of magnetic data for this powdered sample, and as such, the molecular weight was actually less than that used to calculate molar susceptibilities.

The electronic spectrum of $(PPh_4)[Fe(bpy)(Cl_4Cat)_2]$ is dominated by a single broad, intense transition centered at 595 nm with a molar extinction coefficient of 6×10^3 M^{-1} cm^{-1} in acetone solution. The band shows only a slight solvatochromic effect, varying in position from 610 nm in chloroform to 592 nm in acetonitrile.

Electronic Structure of the $Fe(bpy)(Cl_4Q)_2^n$ (n = +1, 0, −1) Series. The magnetic properties and Mossbauer spectra measured for members of the $Fe(bpy)(Cl_4Q)_2^n$ series, with n = 0 and −1, indicate that through the series the central metal remains as a high-spin ferric ion and that redox activity through the series occurs at the quinone ligands. The unusually short C–O bond lengths found for both structures may result from an unusual π-bonding effect with Fe(III), but other structural studies will be required to identify this as a general feature of Fe–Cat bonding in the bis(catecholato)iron(III) species. Characterization on members of the $Cr(bpy)(SQ)_2^+$ series,[19] the $Ru(bpy)(SQ)_2^+$ series,[38] and related iron(III)–semiquinone[17,18] complexes leads us to conclude that oxidation of Fe(bpy)(SQ)(Cat) would also occur at the catecholate ligand to give a product with the $Fe(bpy)(SQ)_2^+$ charge distribution. Our experience with the silver ion oxidation of Fe(bpy)(DBSQ)(DBCat) perhaps indicates that the cationic complexes may be unstable with respect to disproportionation to $Fe(bpy)_3^{3+}$ and $Fe(DBSQ)_3$. Nevertheless, in a species of this form it may be anticipated that the semiquinone ligands would be antiferromagnetically coupled with the $S = {}^5/_2$ iron in a complex of this form to give a $S = {}^3/_2$ ground state.

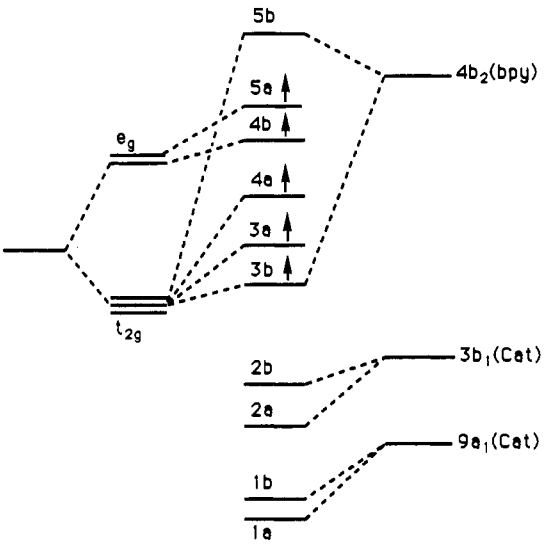

Figure 6. Orbital diagram for $Fe(bpy)(Cat)_2^-$ based on molecular orbital calculations carried out on the chromium analogue.[44]

Fenske–Hall calculations have been used to provide information on the electronic structure of the $Cr(bpy)(SQ)_2^+$–$Cr(bpy)(SQ)(Cat)$–$Cr(bpy)(Cat)_2^-$ redox series.[44] The results of these calculations may be used to understand the electronic structure of the iron analogues. Figure 6 shows the electronic levels obtained from the calculation on $Cr(bpy)(Cat)_2^-$ adapted to the iron analogue by addition of the octahedral e_g level to accommodate the two additional electrons of the high-spin ferric ion. A feature of this diagram that is of interest is the placement of filled catecholate π-levels at energies below the metal d-orbitals. This provides a configuration that is in accord with the Mossbauer and magnetic properties of the anion. The transition at 595 nm, which, from the orbital diagram, can be assigned as a LMCT band in accord with the absence of a significant solvatochromic effect, corresponds to a transition from the catecholate 2b level to the 3b level, which is primarily metal in character. However, it is also clear from properties of the neutral complex that oxidation occurs from a catecholate π-level that is lower in energy than the iron 3d levels to give the mixed-charge ligand complex.

A continuing interest in our studies on iron complexes containing the quinone ligands is the identification of species that may show intramolecular iron–quinone electron transfer related to that of $Co(bpy)(DBSQ)(DBCat)$.[45] The orbital diagram in Figure 6 provides insights into parameters that may influence the balance of charge between the metal and quinone ligand. Electron-withdrawing substituents on the catecholate ligand would serve to increase the separation between metal and quinone π-levels, shifting the LMCT band to higher energy. Examples of anionic complexes are not available for this comparison, but the neutral Fe(bpy)(SQ)(Cat) series shows this effect quite clearly. Two overlapped transitions appear at low energy for the phenanthrenequinone, 3,5-di-*tert*-butylquinone, and tetrachloroquinone complexes with the PhenQ and DBQ complexes showing transitions that are shifted solidly into the near-IR relative to the Cl_4Q analogue. Counter-ligand bonding also may contribute in a significant way to the metal–quinone orbital energy separation through coupling with an electronic level that would otherwise

(44) Gordon, D. J.; Fenske, R. F. *Inorg. Chem.* **1982**, *21*, 2907.
(45) Buchanan, R. M.; Pierpont, C. G. *J. Am. Chem. Soc.* **1980**, *102*, 4951.

be strictly metal in character. This appears in the diagram in Figure 6 as a coupling interaction between the bipyridine π-level and one of the metal orbitals (3b). Strong counter-ligand π-bonding effects may serve to decrease the 3b-2b separation. This appears for the Fe(bpy)(DBSQ)(DBCat) and Fe(en)(DBSQ)-(DBCat) complexes as a shift of 100 nm in the lowest energy transition, with this transition appearing at higher energies for the ethylenediamine complex. The only other well-characterized monomeric anionic complex of this series, $Fe(acac)(RCat)_2^-$ (R = $CONHCH_2CO_2Et$),[11] also shows evidence of this effect relative to $Fe(bpy)(Cl_4Cat)_2^-$. Ligand substituent effects contribute to this comparison, but the transition that appears to correspond to the 595-nm band of the bipyridine complex appears at 537 nm for $Fe(acac)(RCat)_2^-$. Fenske's calculations on the $Cr(bpy)(Q)_2$ series show in a dramatic way how metal and quinone orbital energies depend upon the overall charge of the complex. Oxidation of $Cr(bpy)(Cat)_2^-$ to the $Cr(bpy)(SQ)_2^+$ cation results in stabilization of the metal d orbitals with a slight increase in the energy of the quinone π-levels. The effect of this is that increased mixing between metal and quinone levels occurs and, upon oxidation, levels that are largely localized metal and ligand orbitals become separated by only tenths of electronvolts in energy. How this carries over to the related iron series is unclear, but it may be anticipated that the members of the redox series with the closest metal and quinone orbital energy separation will be cationic in charge.

Acknowledgment. Research at the University of Colorado was supported by the National Institutes of Health (Grant No. GM-23386) and the National Science Foundation (Grant No. CHE 88-09923); research carried out at the University of California was supported by the National Institutes of Health (Grant No. HL-13652).

Registry No. $Fe(bpy)(Cl_4SQ)(Cl_4Cat)$, 138666-82-7; $Fe(Cl_4SQ)_3$, 68846-32-2; $(PPh_4)[Fe(bpy)(Cl_4Cat)_2]$, 138666-84-9; $(CoCp_2)[Fe(bpy)(Cl_4Cat)_2]$, 138666-85-0; $(PPh_4)[Fe(bpy)(Cl_4Cat)_2]\cdot CH_2Cl_2$, 138666-86-1; $Fe(OPPh_3)(Cl_4CatH)(Cl_4Cat)\cdot C_3H_7OH$, 138666-88-3; $Fe(bpy)(Cl_4SQ)_2^+$, 138666-89-4.

Supplementary Material Available: Tables of magnetic susceptibility data for $Fe(bpy)(Cl_4SQ)(Cl_4Cat)$ and $(PPh_4)[Fe(bpy)(Cl_4Cat)_2]$ and, for $(PPh_4)[Fe(bpy)(Cl_4Cat)_2]$ and $Fe(OPPh_3)_3(Cl_4CatH)(Cl_4Cat)$, tables giving crystal data and details of the structure determinations, anisotropic thermal parameters, hydrogen atom locations, and bond lengths and angles and diagrams showing intermolecular packing interactions (32 pages); tables of structure factors (21 pages). Ordering information is given on any current masthead page.

Contribution from the Department of Chemistry, Birkbeck College, University of London, Gordon House and Christopher Ingold Laboratories, 29 Gordon Square, London WC1H 0PP, U.K.

Studies of Platinum(II) Methionine Complexes: Metabolites of Cisplatin[1]

Richard E. Norman,[2] John D. Ranford, and Peter J. Sadler*

Received June 13, 1991

Reactions of L-methionine (L-MetH) with $[PtX_4]^{2-}$ (X = Cl, Br, I) in 1:1 and 2:1 mole ratios have been studied in aqueous solutions at pHs from 1.9 to 8.7 using ^1H, ^{13}C, ^{15}N, and ^{195}Pt NMR spectroscopy. Some related reactions of L-ethionine, and D-methionine methyl ester were also studied. For $[Pt(L\text{-}MetH\text{-}S,N)Cl_2]$, two diastereomers were characterized, one present in ca. 10% excess, the major form having an approximate envelope ring conformation and the minor form being a flattened boat, whereas in the crystalline state both isomers have the same ring conformation. The carboxylate group of the diastereomers (pK_a 2.57) does not coordinate under these conditions. The value of $\Delta G^{\ddagger}$ (74.6 kJ mol^{-1}, 337 K) for S inversion is higher than that for nonchelated analogues. At low pH (ca. 2), the predominant form of the 2:1 complex is the partially-ring-opened species *cis*-$[Pt(L\text{-}MetH\text{-}S,N)(L\text{-}MetH_2\text{-}S)Cl]^{2+}$. This transforms reversibly into ring-closed forms at neutral pH, and of these *cis*-$[Pt(L\text{-}Met\text{-}S,N)_2]$ predominates by about 10:1 over *trans*-$[Pt(L\text{-}Met\text{-}S,N)_2]$. For both of these ring-closed species, the three possible diastereomers (*R,R*: *R,S*/*S,R*; *S,S*) are resolved in ^{195}Pt NMR spectra. The 2:1 complexes are thought to be metabolites of the anticancer drug cisplatin. Reactions of cisplatin, *cis*-$[PtCl_2(NH_3)_2]$, and *cis*-$[Pt(NH_3)_2(H_2O)_2]^{2+}$ with L-methionine in 1:1 and 1:2 mole ratios, at pH 2-7, were also studied. The assignments of ^{15}N and ^{195}Pt resonances were greatly aided by the use of various combinations of natural abundance ^{14}N and ^{15}N enrichment in both ammonia and methionine. For 1:1 reactions with cisplatin, the major products are $[Pt(L\text{-}Met\text{-}S,N)(NH_3)_2]^+$, *cis*- and *trans*-$[Pt(L\text{-}Met\text{-}S,N)(NH_3)Cl]$, and the three diastereomers of *cis*-$[Pt(L\text{-}Met\text{-}S,N)_2]$, and for the 1:2 reactions the products are the diastereomers *R,R*-, *R,S*/*S,R*-, *S,S*-*cis*-$[Pt(L\text{-}Met\text{-}S,N)_2]$, together with minor amounts of *R,R*-, *R,S*/*S,R*-, *S,S*-*trans*-$[Pt(L\text{-}Met\text{-}S,N)_2]$.

Introduction

The amino acid methionine[3] (L-MetH) may play an important role in the metabolism of platinum anticancer drugs both in vivo and in cell culture media. Methionine-containing Pt(II) metabolites have been identified in the urine of patients receiving *cis*-$[PtCl_2(NH_3)_2]$ therapy.[4] As well, Pt(II)-methionine complexes form rapidly in plasma after injection of cisplatin into rats,[5] and methionine appears to enhance the nephrotoxicity of cisplatin.[6] Various attempts have been made to characterize Pt(II)-methionine complexes by HPLC methods.[5,7] Ammonia release

(1) Portions of this work were presented at the following. The 1989 International Chemical Congress of Pacific Basin Societies, Honolulu, HI, 1989; BIOS 88. (b) SAMBAS III, Bosen, Germany, 1990; Abstr. 019, p 73.

(2) Present address: Department of Chemistry, Duquesne University, Pittsburgh, PA 15282.

(3) Abbreviations used: L-MetH, L-methionine; D-Met-Me, D-methionine methyl ester; L-EthH, L-ethionine; en, 1,2-diaminoethane; pH*, pH meter reading in D_2O solution; TSP sodium 3-(trimethylsilyl)-2,2,3,3-tetradeuteriopropanoate. Where there is ambiguity, the terms cis and trans refer to like coordinated atoms (e.g. N's of L-MetH and NH_3). A primed complex (e.g. **1A'**) differs from an unprimed complex (**1A**) by removal of protons from (uncoordinated) carboxyl groups of methionine.

(4) (a) Repta, A. J.; Long, D. F. In Cisplatin; Current Status and New Developments; Prestayko, A. W., Crooke, S. T., Carter, S. K., Eds.; Academic Press: New York, 1980; pp 285-304. (b) Riley, C. M.; Sternson, L. A.; Repta, A. J.; Slyter, S. A. *Anal. Biochem.* **1983**, *130*, 203-214. (c) Sternson, L. A.; Repta, A. J.; Shih, H.; Himmelstein, K. J.; Patton, T. F. In *Platinum Coordination Complexes in Chemotherapy*; Hacker, M. P., Douple, E. B., Krakoff, I. H., Eds.; Martinus Nijhoff: Boston, MA, 1984; pp 126-137.

(5) Daley-Yates, P. T.; McBrien, D. C. H. *Biochem. Pharmacol.* **1984**, *33*, 3063-3070.

(6) Alden, W. W.; Repta, A. J. *Chem. Biol. Interact.* **1984**, *48*, 121-126.

(7) De Waal, W. A. J.; Maessen, F. J. M. J.; Kraak, J. C. *J. Chromatogr.* **1987**, *407*, 253-272 and references therein.

0020-1669/92/1331-0877$03.00/0